

SUPPLEMENTAL INFORMATION

Vapor Sensing Characteristics of Nanoelectromechanical Chemical Sensors Functionalized Using Surface-Initiated Polymerization

Heather C. McCaig, Ed Myers, Nathan S. Lewis, Michael L. Roukes

I. Method Details

II. Vapor Exposure Data

III. Calculation of Partition Coefficients

IV. Ellipsometry of Film Swelling

V. Extended (5000 s) Exposures to Vapors

VI. Sensor to Sensor Repeatability of Responses to Analyte Vapors

I. METHOD DETAILS

A. Materials

Methyl methacrylate (10-100 ppm MEHQ inhibitor), HQ/MEHQ inhibitor removal column packing, and poly(methyl methacrylate) (PMMA; $T_g=105\text{ }^\circ\text{C}$; $MW = 35,000$; $\rho = 1.20\text{ g mL}^{-1}$) were purchased from Scientific Polymer Products, Inc. Bis(2-[2'-bromoisobutyryloxy]ethyl)disulfide (BiBOEDS) (>90%) was purchased from ATRP Solutions. Methanol (anhydrous, 99.8%), copper (I) bromide (CuBr) (98%) and 2,2'-bipyridyl (>99%) were purchased from Aldrich. CuBr was purified by stirring with glacial acetic acid for 24 h at room temperature, followed by rinsing with ethanol and diethyl ether, and then drying overnight in vacuum. Purified CuBr was stored in a vacuum desiccator until use. Absolute ethanol was purchased from Decon Laboratories, Inc. Regent grade hexane, heptane, toluene, ethyl acetate, chloroform, tetrahydrofuran, isopropanol, and carbon tetrachloride were purchased from VWR, and were used to produce analyte vapors. All chemicals were used as received unless otherwise stated. Ultrapure, deionized water (18 M Ω cm resistivity) was used for all syntheses.

B. Nanocantilevers

The fabrication of silicon nitride nanocantilevers with integrated piezoresistive readouts has been described in detail previously.^{1, 2} Briefly, cantilever and bond-pad shapes were patterned with electron-beam lithography onto a 100 nm thick SiN layer on a silicon substrate, followed by gold film deposition, and then liftoff. Dry plasma etching was then used to release the cantilevers. The gold overlayer served as both an etch mask during fabrication and later as a piezoresistive transducer.³ Nanocantilevers had a typical fundamental resonance frequency of 10-12 MHz, quality (Q) factors of 100-200 in ambient conditions, and a capture area of 1.5 μm^2 . The resonance was actuated thermoelastically.⁴ Nanocantilever sensors were operated with

home-built, LabView controlled, electronics³ that tracked each sensor's resonance frequency using parallel, independent phase-locked loops.

C. Initiator SAM Formation

Substrates were cleaned by sequential rinses with hexane, acetone, tetrahydrofuran, methanol, and absolute ethanol, followed by a UV/ozone plasma clean (Samco UV-1) for 8 min with a stage temperature of 65 °C. After rinsing with deionized water and thoroughly drying with a stream of compressed air, the substrates were immersed into a 5 mM solution of initiator in absolute alcohol. For a single chip, 2.5 mL of the solution (15 mg initiator), in a 20 mL scintillation vial was sufficient to fully immerse the substrate. The sealed vials were stored into the dark for 24-48 h to ensure the formation of a dense and ordered self-assembled monolayer (SAM).

D. Polymerization

Polymerization of MMA was performed by water-accelerated SI-ATRP.⁵ Neat MMA was first passed through an inhibitor removal column. The purified MMA was either used immediately, or was stored in sealed vials that were placed in a freezer until use. A two-necked round bottom flask was charged with 7.5 mg of purified MMA, 6 mL methanol, and 1.5 mL deionized water. The flask was sealed with septa and then the solution was sonicated while sparging for 45 min with N₂(g) or Ar(g). The catalyst components, 258 mg of CuBr and 114 mg 2-bipy, were then added to the solution, and the solution was then simultaneously sonicated and sparged until the catalyst dissolved, which generally took 30-45 min. Substrates were suspended with a flat alligator clip in a 20 mL scintillation vial equipped with a small stir bar and a septum. The clip was attached to a wire that was sufficiently long to bend over the rim of the vial, and was held in place with the septum. The vial was purged with N₂(g) or Ar(g) for at least 45 min before introduction of the solution. To minimize contact with oxygen, the reaction solution was transferred via syringe from the round-bottom flask to the vial that contained the suspended substrate. The reaction was allowed to proceed at room temperature with stirring and a constant inert gas purge. At the desired time, the substrate was removed and thoroughly rinsed sequentially with tetrahydrofuran, methanol, and absolute ethanol, respectively.

E. Polymer Film Characterization

Films were characterized using ellipsometry and scanning-electron microscopy (SEM). Flat substrates for ellipsometric measurements were prepared by evaporating 3 nm of chromium, followed by 30 nm of gold, onto a silicon wafer that had been coated with a native oxide layer. The cleaning, SAM formation, and polymerization procedures were identical to those used for the nanocantilevers. The PMMA film thickness was measured using a Gaertner L166C ellipsometer, equipped with a He-Ne (633 nm wavelength) laser, at a 70° angle of incidence. The optical

constants of the flat gold substrates were measured prior to formation of the initiator SAM. The thickness was determined for both the initiator SAM and the polymer film. The refractive index of the SAM was assumed to be 1.46, and the refractive index of the PMMA film was assumed to be 1.49.⁶ The thickness of the initiator SAM was 0-2 Å. SEM (ZEISS 1550 VP FESEM and FEI Sirion) images were used to verify the quality of nanocantilever fabrication as well as the quality of the SI-ATRP grown polymer films.

F. Drop-cast Polymer Films

PMMA solutions for drop-casting were formed by first making a concentrated solution by sonicating ~ 100 mg of PMMA in 20 mL toluene, until the polymer beads had dissolved. This concentrated solution was diluted to 5 mM of PMMA. A 10 µL micropipette was used to apply a 1.5 µL droplet of the dilute PMMA solution to the chip that contained the nanocantilever sensors, and the solvent was then allowed to evaporate.

G. Vapor Exposures Experiments

Nanocantilevers were exposed to analyte vapors using an automated vapor delivery system controlled by LabView.⁷ At least three sensors of each type (bare, dropcast PMMA, SI-ATRP PMMA) were tested. The analytes (hexane, toluene, heptane, ethyl acetate, chloroform, tetrahydrofuran, and isopropanol) were delivered at concentrations of 0.005-0.08 P/P^0 (partial pressure divided by saturated vapor pressure), and each exposure consisted of 70 s of pure carrier gas, 400 s of analyte vapor exposure, followed by 630 s of carrier gas to purge the system. For single concentration experiments, a run consisted of five exposures to each analyte at $P/P^0 = 0.020$. For linearity experiments, five exposures per concentration per analyte were delivered in the order $P/P^0 = 0.030, 0.010, 0.0480, 0.0050, 0.080, \text{ and } 0.020$, to prevent possible hysteresis from affecting the linearity profile. The nanocantilevers were housed in a brass chamber with an internal volume of 100 mL. Between one and four sensors were tested in each experimental run, and prior to data collection all of the sensors were conditioned by multiple exposures to each analyte. The temperature was not controlled, but was stable at 21 ± 1 °C.

H. Data Analysis

The nanocantilever frequency data were corrected for baseline drift prior to extraction of the sensor responses. The baseline noise was computed as the standard deviation of the drift-corrected baseline frequency over a period of 10 s prior to the sensor response. The signal-to-noise ratio was calculated as the average response divided by three times the baseline noise. Data analysis was performed using OriginLab (Version 7.5). The nanocantilever sensor response data reported in the figures and tables were recorded from single, representative sensors. Some

variation was observed between individual sensors of each type, but the variation did not distort the reported trends.

II. VAPOR EXPOSURE DATA

A. Figures of Cantilever Frequency Measurements for 0.02 P/P^0 Vapor Exposures:

The following figures show baseline-drift-corrected frequency traces for three cantilever sensors with different surface functionalizations: bare gold (S1), a drop-cast PMMA film (S2), and a SI-ATRP-grown PMMA film (S3). Each figure depicts the response of a single sensor to a series of exposures to analyte vapors at a concentration of $P/P^0 = 0.020$. For these experiments, five sequential exposures to each of seven vapors were conducted in the order hexane, toluene, heptane, ethyl acetate, chloroform, isopropanol, and tetrahydrofuran.

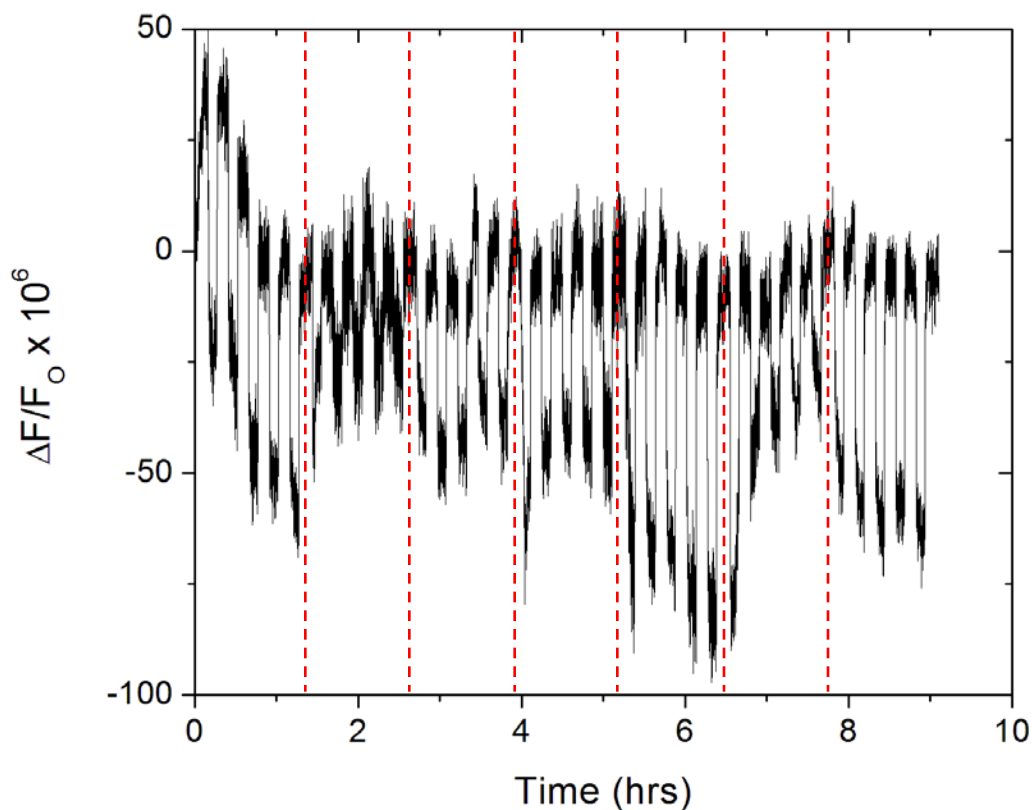


Figure S1: Responses of a bare cantilever to a series of analyte vapors delivered at $P/P^0 = 0.020$. The dashed red lines denote a change of analyte.

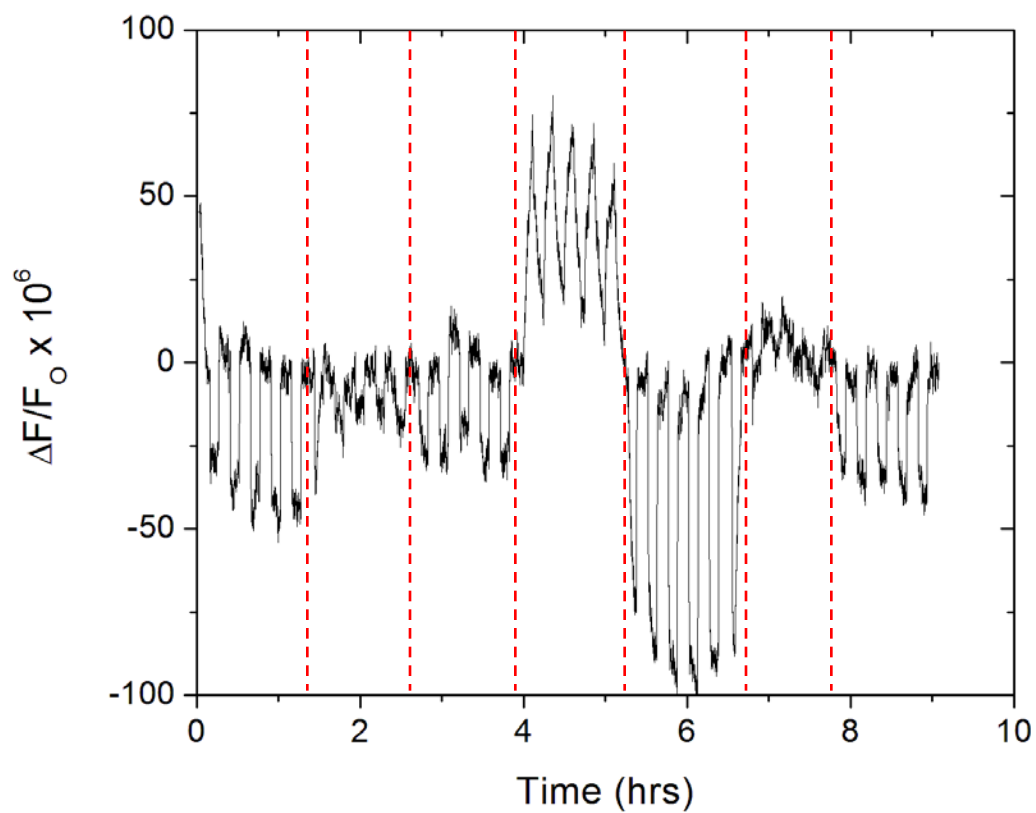


Figure S2: Responses of a cantilever functionalized with a drop-cast film of PMMA to a series of analyte vapors delivered at $P/P^0 = 0.020$. Functionalization of the cantilever with a drop-cast polymer film introduced selectivity and enhanced the sensitivity relative to a bare sensor. The dashed red lines denote a change of analyte.

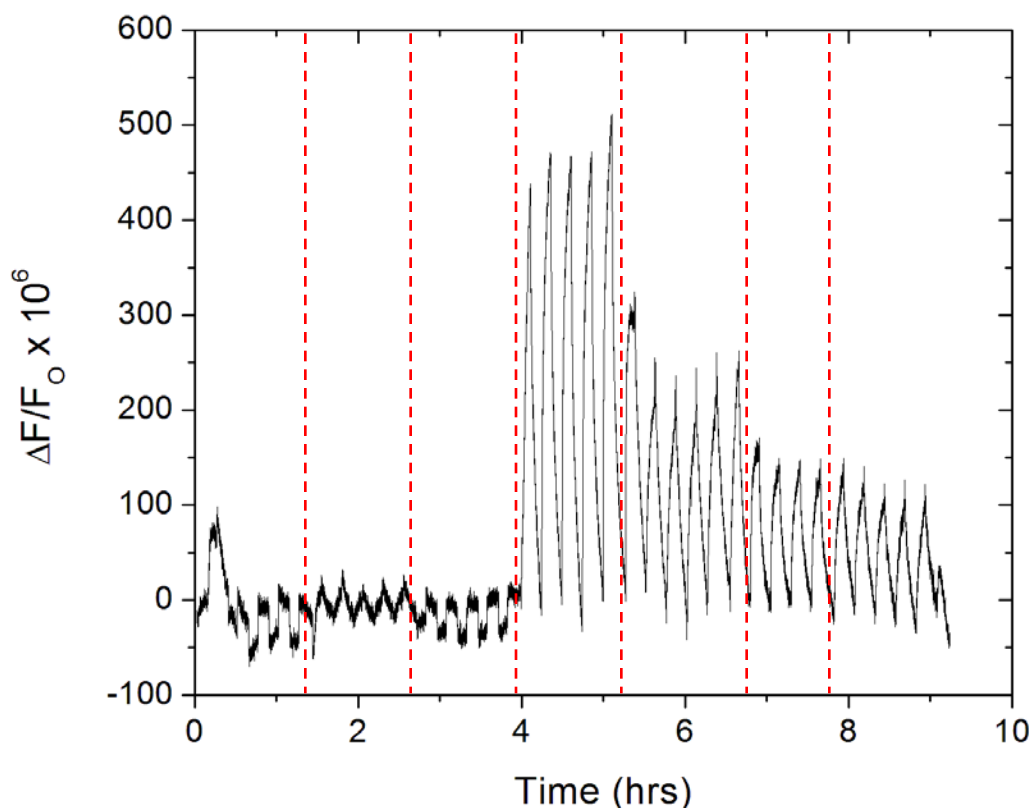


Figure S3: Responses of a cantilever functionalized with an SI-ATRP grown PMMA film to a series of analyte vapors delivered at $P/P^0 = 0.020$. The sensor's responsivity to polar vapors was greatly enhanced relative to a cantilever that had instead been functionalized with a drop-cast PMMA film. The dashed red lines denote a change of analyte.

B. Tabulated Responses Data

Table S1: Relative frequency shifts (a) and signal-to-noise ratio (b) for nanocantilevers with a bare gold surface, a dropcast PMMA film, and a SI-ATRP PMMA film exposed to 400 s pulses of various analyte vapors.

Analyte	(a) $\Delta f_{max}/f_0 \times 10^6$		
	Bare	Drop-cast PMMA	SI-ATRP PMMA
Hexane	-56.89 ± 3.34	-39.71 ± 4.63	-42.37 ± 2.62
Toluene	-22.96 ± 2.79	-13.73 ± 1.87	18.94 ± 5.45
Heptane	-33.02 ± 2.93	-26.83 ± 2.94	-31.67 ± 2.39
Ethyl Acetate	-40.45 ± 2.43	-52.31 ± 7.09	478.36 ± 26.47
Chloroform	-60.53 ± 9.34	-74.28 ± 6.29	219.21 ± 39.51
Isopropanol	-33.86 ± 9.22	-13.28 ± 2.52	149.13 ± 10.28
Tetrahydrofuran	-48.22 ± 4.55	-28.16 ± 1.83	126.52 ± 11.27

(b) SNR			
Analyte	Bare	Dropcast PMMA	SI-ATRP PMMA
Hexane	9.8 ± 0.6	6.9 ± 0.8	4.6 ± 0.05
Toluene	4.0 ± 0.5	2.4 ± 0.3	1.1 ± 0.1
Heptane	5.7 ± 0.5	4.6 ± 0.5	3.1 ± 0.3
Ethyl Acetate	7.0 ± 0.4	9.1 ± 1.2	49.6 ± 1.1
Chloroform	10.4 ± 1.6	12.9 ± 1.1	24.2 ± 1.1
Isopropanol	5.8 ± 1.6	2.3 ± 0.4	17.2 ± 2.0
Tetrahydrofuran	8.3 ± 0.8	4.9 ± 0.3	13.5 ± 0.6

C. Equilibrium Response to Polar Vapors

When cantilevers coated with PMMA grown using SI-ATRP were exposed to polar vapors, an initial period (~ 15 min) of rapid increase in frequency was observed. This period was followed by a transition to a slower rate of increase that continued for > 1 h before the sensor reached steady-state. Non-Fickian diffusion, characterized by an initial mass loading that is followed by a delayed relaxation of the polymer chains, commonly occurs in glassy polymers such as PMMA, which may explain the shape of the responses to polar vapors of cantilevers that had been coated with PMMA grown using SI-ATRP.⁸⁻¹³

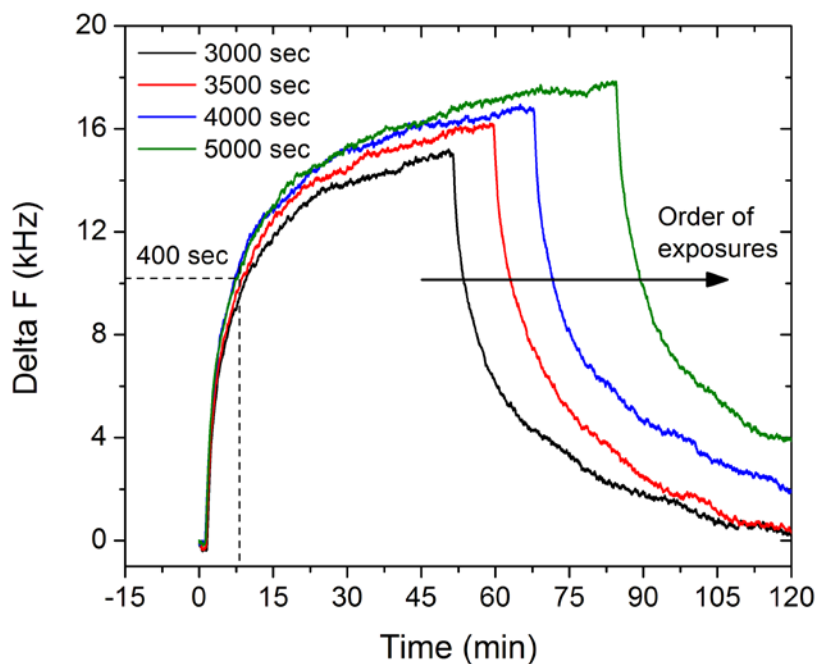


Figure S4: A cantilever coated with PMMA grown using SI-ATRP exposed to ethyl acetate vapor ($P/P^0 = 0.020$) required long exposure times to reach equilibrium with polar vapors.

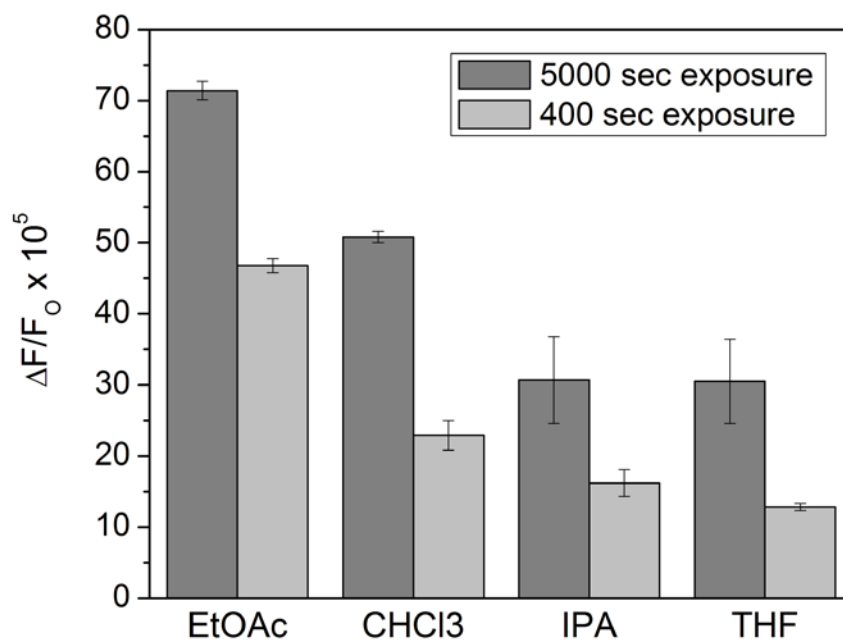


Figure S5: Comparison of the responses of cantilevers coated with PMMA grown using SI-ATRP to polar vapors exposed for 400 s and 5000 s.

Table S2: Equilibrium responses of a nanocantilever coated with PMMA grown using SI-ATRP, along with the percentage increase in response magnitude compared to the sensor response generated by a 400 s pulse of analyte vapor.

SI-ATRP PMMA Equilibrium Responses		
Analyte	$\Delta f_{max}/f_0 \times 10^6$	Percent increase in response magnitude
Ethyl Acetate	714.73 ± 13.21	53%
Chloroform	508.05 ± 7.85	122%
Isopropanol	307.83 ± 61.40	90%
Tetrahydrofuran	305.51 ± 59.68	138%

III. PARTITION COEFFICIENTS FOR DROPCAST AND SI-ATRP GROWN PMMA FILMS

A. Method for Determining Partition Coefficients

Partition coefficients (K_{eq}) were determined by measurement of the mass uptake of PMMA films applied to quartz-crystal microbalances (QCMs). Each QCM was cleaned by sequential rinses with hexane, acetone, and methanol, before measurement of the initial resonance frequency, $F_{0,i}$. PMMA films were prepared either by spray coating the QCM with a solution of PMMA (Scientific Polymer Products, Inc.) in tetrahydrofuran (160 mg / 20 mL) using an airbrush, or by SI-ATRP, as described above. All PMMA films were stored in a closed, but not sealed, container for at least 24 h after film formation, to aid in the evaporation of any trapped solvent. Before data collection, QCMs were conditioned by exposure to a randomized series of vapor exposures for 12-18 h.

The QCMs were exposed to analyte vapors with an automated vapor delivery system.⁷ Five exposures of the seven vapors at each of the five concentrations ($P/P^0 = 0.010, 0.020, 0.040, 0.060, 0.080$) were conducted in an order randomized for both analyte identity and concentration. After an initial purge of 500 s, each exposure was 400 s in duration, with a 700 s purge between exposures. The change in resonance frequency due to polymer coating, $\Delta F_{polymer}$, was calculated as the difference between the resonance frequency before and after coating. The frequency change due to each vapor exposure, $\Delta F_{analyte}$, was calculated as the difference in frequency between the QCM during exposure relative to the baseline frequency. The baseline frequency was calculated as the average frequency during the 20 s prior to the specific vapor exposure, and the frequency during exposure was calculated as the average frequency between 350 and 398 s after the exposure had begun.

The calculation of the partition coefficient from the QCM frequency shift data has been described previously.¹⁴ Briefly, a line with a forced zero was first fitted versus the data as a function of analyte concentration. The slope of this fit was then converted into a partition coefficient using:

$$K_{eq} = \frac{\rho R T m * 10^6}{M_w \Delta f_{polymer} P_{atm}}$$

where R is the ideal gas constant ($1 \text{ atm mol}^{-1} \text{ K}^{-1}$), ρ is the density (g mL^{-1}) of the polymer, T is the temperature (K), m is the slope of $\Delta F_{analyte}$ versus concentration (Hz/ppth in air), M_w is the molecular weight (g mol^{-1}) of the analyte, $\Delta F_{polymer}$ (Hz) is the frequency shift due to the polymer coating, and P_{atm} is the atmospheric pressure (atm). The density of PMMA used in the K_{eq} calculations was 1.20 g mL^{-1} for QCMs that had both spray-coated and SI-ATRP-grown PMMA films.

B. Tabulated Partition Coefficients

Table S3: Calculated partition coefficients for bulk and SI-ATRP PMMA films.

Partition Coefficients (K_{eq})		
Analyte	Spray-Coated Bulk PMMA	SI-ATRP PMMA
Hexane	65	40
Toluene	540	375
Heptane	175	90
Ethyl Acetate	390	280
Chloroform	245	200
Isopropanol	415	350
Tetrahydrofuran	160	115

IV. ELLIPSOMETRY OF POLYMER FILM SWELLING

A. Method

Substrates coated with either a drop-cast or SI-ATRP-grown PMMA film were placed into a vapor exposure chamber that was situated on the sample stage of the ellipsometer. The vapor exposure chamber consisted of a plastic box with ports for the laser beam as well as the vapor stream input. A glass window made from a microscope slide cover slip was installed in the top of the chamber to allow for substrate alignment. Saturated analyte vapor was generated by passing a stream of laboratory air through a bubbler. A manual valve was used to switch the gas stream flowing through the sensor chamber between laboratory air and saturated analyte vapor.

Substrates for measurement of the swelling of drop-cast and SI-ATRP-grown PMMA films were QCMs that had been previously used to determine K_{eq} of the SI-ATRP grown film. The baseline film thickness of each sample was measured after exposure to a flow of laboratory air for 2 min. The flow was then switched to a stream of saturated analyte vapor for 6 min, and the film thickness was measured again. This procedure was repeated three times for each vapor.

B. Polymer Film Swelling Data

The relative vertical swelling of the SI-ATRP-grown PMMA film did not match the observed trend of enhanced nanocantilever sensor responses to polar vapors.

Table S4: Relative swelling of SI-ATRP PMMA films exposed to saturated analyte vapors.

Relative Swelling ($\Delta H/H \times 10^5$)	
Analyte	SI-ATRP PMMA
Hexane	0.01
Toluene	0.12
Heptane	0.04
Ethyl Acetate	0.20
Chloroform	1.26
Isopropanol	0.18
Tetrahydrofuran	0.34

The ratio of the relative vertical film swelling to the partition coefficient was also determined, and the comparison of vertical film swelling to mass loading did not match the observed trend of enhanced nanocantilever responses to polar vapors.

Table S5: Ratio of relative swelling to partition coefficient of SI-ATRP PMMA for various analyte vapors.

Relative Swelling ($\Delta H/H$)/$K_{eq} \times 100$	
Analyte	SI-ATRP PMMA
Hexane	2.5
Toluene	3.3
Heptane	4.3
Ethyl Acetate	7.0
Chloroform	63.3
Isopropanol	5.2
Tetrahydrofuran	29.7

V. EXTENDED (5000 s) EXPOSURES TO VAPORS

The steady-state response of the functionalized sensors to polar analyte vapors required 53 -138 % longer than a 400 s exposure. Furthermore, even after 5000 s exposures to ethyl acetate and isopropanol, cantilevers coated with PMMA grown by Si-ATRP exhibited a nonlinear concentration response. At higher concentrations, even a 5000 s exposure was insufficient for the sensor to reach steady-state. The PMMA film also exhibited a pronounced history effect when exposed to ethyl acetate vapor, whereby an exposure to ethyl acetate at $P/P^0 = 0.030$ produced a smaller response than an exposure to ethyl acetate later in the experiment at $P/P^0 = 0.020$ (Figure S6).

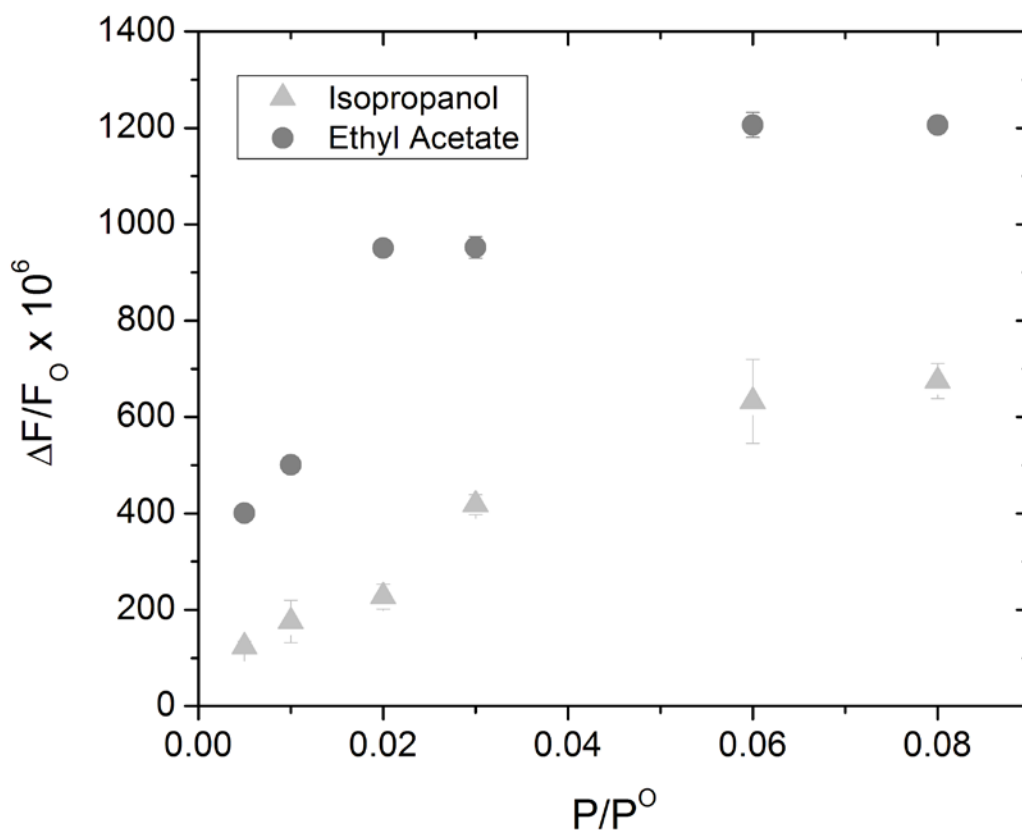


Figure S5: Longer exposure times (5000 s) to polar analyte vapors did not improve linearity because equilibrium was not reached for high vapor concentrations.

VI. SENSOR TO SENSOR REPEATABILITY OF RESPONSES TO ANALYTE VAPORS

Figure S6 shows the responses of two sensors each for drop-cast PMMA and SI-ATRP-coated nanocantilevers. The cantilevers coated with the drop-cast PMMA films were from the same chip. The cantilevers with the SI-ATRP films were also from the same chip, and thus were both coated via the same reaction. The responses data are for sensors that exhibited no obvious defects observed with SEM after the vapor exposure experiments had been completed. Poorly-performing sensors were not used for vapor exposure experiments and were observed in both categories, typically due to occasional fabrication defects, nanocantilevers damaged by debris, or the gluing-down of nanocantilevers upon attempted deposition of drop-cast PMMA films. Poorly-performing sensors exhibited either no resonance due to extreme mechanical failure, or very low quality factors (Q), such that changes in resonance frequency could not be readily measured. Generally, the SI-ATRP coating procedure resulted in a higher yield (no gluing down, and fewer debris) of nanocantilevers that exhibited resonance and acted as good chemical vapor sensors.

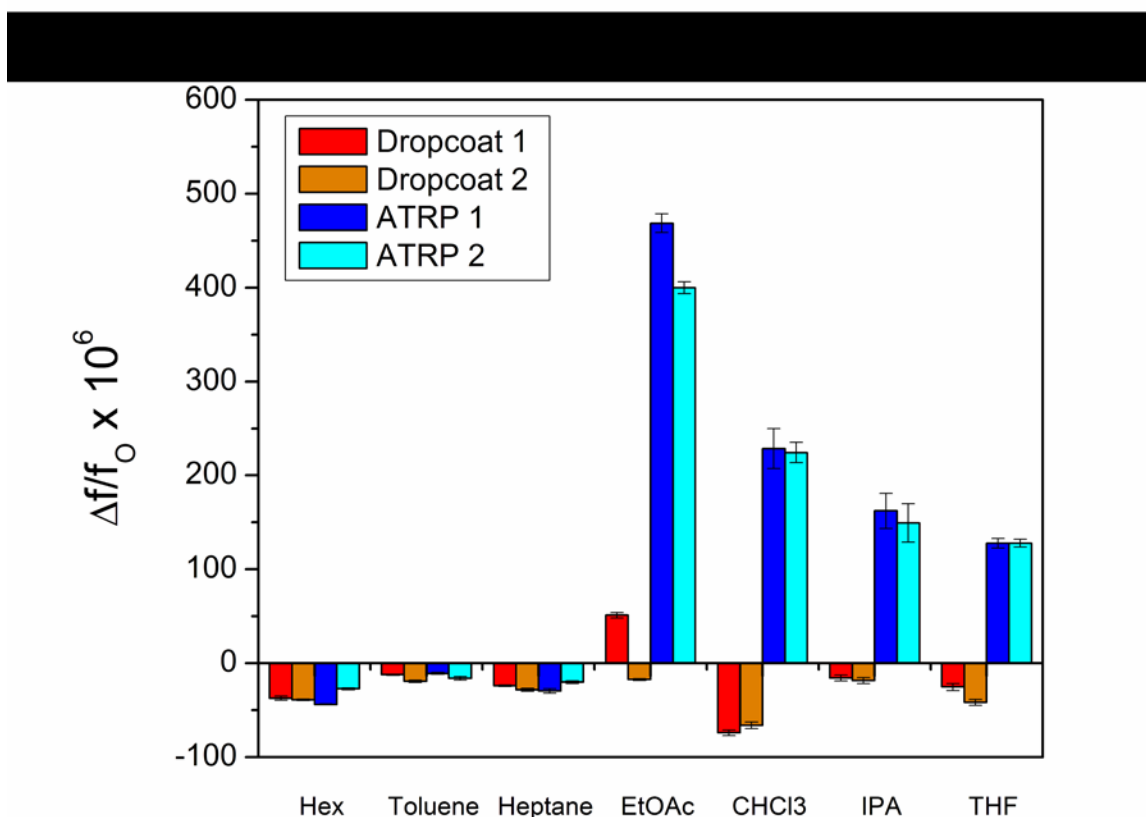


Figure S6: Repeatability of sensor responses to analyte vapors.

REFERENCES

1. Li, M.; Tang, H. X.; Roukes, M. L., *Nat. Nanotechnol.* **2007**, 2 (2), 114-120.
2. Yang, Y. T.; Ekinici, K. L.; Huang, X. M. H.; Schiavone, L. M.; Roukes, M. L.; Zorman, C. A.; Mehregany, M., *Appl. Phys. Lett.* **2001**, 78 (2), 162-164.
3. Bargatin, I.; Myers, E. B.; Arlett, J.; Gudlewski, B.; Roukes, M. L., *Appl. Phys. Lett.* **2005**, 86 (13), 3.
4. Bargatin, I.; Kozinsky, I.; Roukes, M. L., *Appl. Phys. Lett.* **2007**, 90 (9), 3.
5. Jones, D. M.; Huck, W. T. S., *Adv. Mater.* **2001**, 13 (16), 1256-1259.
6. Kasarova, S. N.; Sultanova, N. G.; Ivanov, C. D.; Nikolov, I. D., *Opt. Mater.* **2007**, 29 (11), 1481-1490.
7. Severin, E. J.; Doleman, B. J.; Lewis, N. S. *Anal. Chem.* **2000**, 72 (4), 658-668.
8. Sfirakis, A.; Rogers, C. E., *Polym. Eng. Sci.* **1981**, 21 (9), 542-547.
9. Berens, A. R.; Hopfenberg, H. B., *J. Membr. Sci.* **1982**, 10, 283-303.
10. Sanopoulou, M.; Petropoulos, J. H., *Macromolecules* **2001**, 34 (5), 1400-1410.
11. Ferrari, M.-C.; Piccinini, E.; Giacinti Baschetti, M.; Doghieri, F.; Sarti, G. C., *Ind. Eng. Chem. Res.* **2008**, 47 (4), 1071-1080.
12. De Angelis, M. G.; Sarti, G. C., *Annu. Rev. Chem. Biomol. Eng.* **2011**, 2 (1), 97-120.
13. Petropoulos, J. H.; Sanopoulou, M.; Papadokostaki, K. G., *Eur. Polym. J.* **2011**, 47 (11), 2053-2062.
14. Briglin, S. M.; Freund, M. S.; Tokumar, P.; Lewis, N. S., *Sens. Actuators B-Chemical* **2002**, 82 (1), 54-74.